DEPARTMENT OF PHYSICS
Institute for Beam Physics and Technology

Stability Improvements at FLUTE
(Verbesserung der Stabilität von FLUTE)

Master thesis
of

Marvin-Dennis Noll

at the Institute for Beam Physics and Technology

Reviewer:	Prof. Dr.-Ing. John Jelonnek (IHM)
Second Reviewer:	Prof. Dr. Anke-Susanne Müller (IBPT)
Advisor:	Dr. Nigel Smale (IBPT)

15.11.2020 – 01.07.2021

Erklärung zur Selbstständigkeit

Ich versichere wahrheitsgemäß, die Arbeit selbstständig angefertigt, alle benutzten Hilfsmittel vollständig und genau angegeben und alles kenntlich gemacht zu haben, was aus Arbeiten anderer unverändert oder mit Abänderungen entnommen wurde und dass ich die Satzung des KIT zur Sicherung guter wissenschaftlicher Praxis in der gültigen Fassung vom 24.05.2018 beachtet habe.

Karlsruhe, den 01.07.2021, _____

Marvin-Dennis Noll

Als Prüfungsexemplar genehmigt von

Karlsruhe, den 01.07.2021, _____

Prof. Dr.-Ing. John Jelonnek (IHM)

Contents

List of Figures

List of Tables

1. Theoretical Framework

1.1 Linear Accelerators

In a linear particle accelerator (LINAC), charged particles such as electrons are accelerated to increase their total energy over their energy at rest.

Compared to heavier particles, such as protons ($m_p = 938.27\,\mathrm{MeV/c^2}$), electrons are fairly light ($m_p = 0.511\,\mathrm{MeV/c^2}$). Therefore they need to be brought to speeds comparable to the speed of light to achieve an useful energy increase. For this reason relativistic mechanics are needed to describe their movements.[1] [1]

With the speed of light $c = 2.998 \times 10^8\,\mathrm{m\,s^{-1}}$ and the particle velocity v, it is common to define [2]:

$$\text{(normalized velocity)} \qquad \beta = \frac{v}{c} \tag{1.1}$$

$$\text{(relativistic mass factor)} \qquad \gamma = \frac{1}{\sqrt{1-\beta^2}} \tag{1.2}$$

The total energy of a particle is

$$U = \underbrace{(\gamma - 1)\, mc^2}_{\text{kinetic engery } W} + \underbrace{mc^2}_{\text{rest energy}} = \gamma mc^2. \tag{1.3}$$

With the kinetic electron energy out of the FLUTE electron gun of $W = 7\,\mathrm{MeV}$, rearranging Equation 1.1 and using in $W = (\gamma - 1)\, mc^2$ yield

$$\gamma = \frac{W}{m_e\, c^2} + 1 = 14.699 \tag{1.4}$$

$$\beta = \sqrt{1 - 1/\gamma^2} = 0.997\,68. \tag{1.5}$$

1.2 Beam Diagnostic Devices for Linear Accelerators

All (linear) particle accelerators need diagnostic devices to monitor the beam sizes, shapes, positions, length or charge.

Beam Position Monitor (BPM)

Faraday Cup

1.3 Signal Analysis

1.3.1 Auto correlation and Cross correlation

The *cross covariance* between two stochastic processes $x[n]$ and $y[n]$ is a measure of the similarity between $x[n]$ at index n_1 and $y[n]$ at index n_2 and is defined as

$$r_{xy}[n_1, n_2] = \mathrm{E}\left\{(x[n_1] - \mu_x[n_1])(y[n_2] - \mu_y[n_2])^*\right\}. \tag{1.6}$$

[1] As relativistic mechanics are a super set of classical mechanics, the equations also apply for slower particles.

For the special case of $y[n] := x[n]$, $r_{xx}[n_1, n_2]$ is called *auto covariance* and is a measure of self similarity of $x[n]$ [3, p. 172].

The processes $x[n]$ and $y[n]$ are called *wide sense stationary* (WSS) if the following two properties hold [3, p. 167]. First, their means $\mu_\xi[n]$ are constant, i.e. they do not depend on the sample index:

$$\mu_x[n] = \mu_x \tag{1.7}$$
$$\mu_y[n] = \mu_y \tag{1.8}$$

Also the auto covariance does not depend on the absolute sample indices n_1 and n_2, but merely on the difference between them:

$$r_{xy}[n_1, n_2] = r_{xy}[m], \qquad \text{with: } m := n_2 - n_1 \tag{1.9}$$

If both process in Equation 1.6 are WSS, Equation 1.6 simplifies to

$$r_{xy}[m] = \mathrm{E}\left\{(x[n] - \mu_x)(y[n-m] - \mu_y)^*\right\}. \tag{1.10}$$

For the auto covariance both means are identical and can be moved outside the expectation operator:

$$r_{xx}[m] = \mathrm{E}\left\{(x[n])(y[n-m])^*\right\} - \mu_x^2. \tag{1.11}$$

When analyzing signals, the stochastic processes are often unknown and only one realization $x[n]$ is known. But if the process generating $x[n]$ is *(weakly) ergodic*, then one realization is enough to determine the auto covariance of the process [4, p. 252]. Then the auto covariance can be estimated with

$$\hat{r}[m] = \frac{1}{N} \sum_{n=m+1}^{N} x[n]\, x^*[n-m] \qquad m \in [0,\, N-1] \tag{1.12}$$

1.3.2 Estimating the Spectrum of a Stochastic Process

For a deterministic, time-discrete signal $x[n] \in \mathcal{L}_1$, the discrete Fourier transform (DFT) exists[5] and is defined as

$$X[k] = \sum_{n=0}^{N-1} x[n]\, \mathrm{e}^{-j\frac{2\pi}{N}k\,n} \qquad k, n \in [0,\, N-1], \tag{1.13}$$

using $k = \frac{N}{2\pi}\,\omega = N\,f$ as the independent, discrete frequency variable. From the complex sequence $X[k]$, often only the magnitude (or energy) is of greater interest while the phase information are neglected. Therefore, S_{xx} is defined as

$$S_{xx} = |X[k]|^2 \tag{1.14}$$

and called the *energy spectral density (ESD)*.

If $x[n]$ is the realization of a stochastic process, then it is of random nature rather than deterministic. Because realizations of physical processes do not posses finite energy, they are not in the $\mathcal{L}_1$ set and their DFT is not defined [6, p. 5].

In this case instead of an energy spectral density, the spectrum of the average power of the process, called the *power spectral density (PSD)*, can be used instead. To compute the PSD, either there are two possibilities:

$$\Phi_{xx}[k] = \sum_{m=-\infty}^{\infty} r[m]\, \mathrm{e}^{-j\frac{2\pi}{N}k\,m} \tag{1.15}$$

$$\Phi_{xx}[k] = \lim_{N\to\infty} \mathrm{E}\left\{\frac{1}{N}\left|\sum_{n=0}^{N-1} x[n]\, \mathrm{e}^{-j\frac{2\pi}{N}k\,n}\right|^2\right\} \tag{1.16}$$

When assuming $r[m]$ decays "fast enough", i.e.

$$\lim_{N\to\infty} \frac{1}{N} \sum_{m=-N}^{N} |m|\ |r[m]| = 0 \tag{1.17}$$

then Equation 1.15 and Equation 1.16 are equal[6, p. 7].

For measured data however neither equations can be used directly. For Equation 1.15 the auto covariance sequence $r[m]$ is unknown. But it could be estimated with Equation 1.12. In case of Equation 1.16 it is not possible to evaluate the limit, because only finite length data can be sampled and also the expectation can not be computed since in general there is only one realization available. Both operations can be neglected when doing an estimation.

With these practical changes in place, Equation 1.15 and Equation 1.16 become

$$\hat{\Phi}_{c,\,xx}[k] = \sum_{m=-(N-1)}^{N-1} \hat{r}[m]\, \mathrm{e}^{-j\frac{2\pi}{N}k\,m} \qquad \text{(Correlogram)} \tag{1.18}$$

$$\hat{\Phi}_{p,\,xx}[k] = \frac{1}{N}\left|\sum_{n=0}^{N-1} x[n]\, \mathrm{e}^{-j\frac{2\pi}{N}k\,n}\right|^2 \qquad \text{(Periodogram).} \tag{1.19}$$

Both methods yield equal results, if $r[m]$ is estimated with the biased estimator $\hat{r}[m]$ in Equation 1.12 in contrast to the unbiased estimator (compare [6, p. 24])

$$\hat{r}_{\text{unbiased}}[m] = \frac{1}{N-m} \sum_{n=m+1}^{N} x[n]\, x^*[n-m] \qquad m \in [0,\, N-1]. \tag{1.20}$$

[7] shows one key weakness of the unmodified periodogram method in Equation 1.19: The variance does not decrease significantly with more samples N. Instead the variance of the periodogram for each frequency approaches the square of the actual PSD:

$$\lim_{N\to\infty} \mathrm{Var}\left\{\hat{\Phi}_{p,\,xx}[k]\right\} = \Phi_{xx}^2[k] \tag{1.21}$$

Furthermore the periodogram/correlogram suffer from the smearing and leakage effects because the limited length of the data samples always causes an implicit windowing, thus reducing frequency resolution.

There are several popular methods that improve on the periodogram/correlogram concepts:

Blackman-Tukey: Because of the poor accuracy of $\hat{r}[m]$ for $k \approx N$ in the definition of $\hat{\Phi}_{c,\,xx}[k]$ and the bigger the N, the more small errors in $\hat{r}[m]$ sum up, truncating/windowing of $\hat{r}[m]$ with $w[k]$ (length M) can be beneficial for the accuracy of the estimation.

$$\hat{\Phi}_{BT,\,xx}[k] = \sum_{m=-(M-1)}^{M-1} w[k]\hat{r}[m]\, \mathrm{e}^{-j\frac{2\pi}{N}k\,m} \tag{1.22}$$

The choice of the window $w[k]$ trades frequency resolution for variance and smearing for leakage reduction [6, p. 41].

Barlett: The Barlett method reduces the variance of the periodogram by splitting the N data samples in $Q = {}^{N}/_{M}$ blocks and averaging together the sub-periodograms:

$$\hat{\Phi}_{q,\,xx}[k] = \frac{1}{M}\left|\sum_{n=0}^{M-1} x_q[n]\, \mathrm{e}^{-j\frac{2\pi}{M}k\,n}\right|^2 \tag{1.23}$$

$$\hat{\Phi}_{B,\,xx}[k] = \frac{1}{Q}\sum_{q=1}^{Q} \hat{\Phi}_{q,\,xx}[k] \tag{1.24}$$

The variance of the estimation scales with Q [7, p. 6]:

$$\mathrm{Var}\left\{\hat{\Phi}_{B,xx}[k]\right\} = \frac{1}{Q}\Phi_{xx}^2[k] \tag{1.25}$$

Welch: The Welch method combines splitting the data into Q segments with windowing each segment and allowing the segments to overlap. With $P = {}^1/_M \sum_{n=0}^{M-1} |w[n]|^2$ being the "power'' of the window, the Welch method is computed as

$$\hat{\Phi}_{s,xx}[k] = \frac{1}{MP}\left|\sum_{n=0}^{M-1} x_s[n]\,\mathrm{e}^{-j\frac{2\pi}{M}k\,n}\right|^2 \tag{1.26}$$

$$\hat{\Phi}_{W,xx}[k] = \frac{1}{Q}\sum_{s=1}^{Q}\hat{\Phi}_{s,xx}[k]. \tag{1.27}$$

Compared to the Barlett method, the overlapping of up to 50 % (see [8]) allows increasing Q, thus reducing the variance.

$$\mathrm{Var}\left\{\hat{\Phi}_{W,xx}[k]\right\} = \frac{1}{Q}\Phi_{xx}^2[k] \tag{1.28}$$

In case on a non-stationary signal $x[n]$, one possibility to analyze and display the spectral content is the use of the short time Fourier transform (STFT) and the spectrogram, which is a two dimensional power spectral density function mapping frequency and time to a third coordinate like height, intensity or color.

To calculate the spectrogram, the signal is split into segments with the sliding window $w[n-m]$ for which duration the signal is assumed to be stationary. For each segment at time index m, the periodogram is calculated according to

$$\hat{\Phi}_{xx}[k,m] = \frac{1}{N}\left|\sum_{n=0}^{N-1} w[n-m]x[n]\,\mathrm{e}^{-j\frac{2\pi}{N}k\,n}\right|^2. \tag{1.29}$$

1.4 Feedback Control Systems

Feedback control systems are used to control a dynamic system (plant) in such a way that its output $y(t)$ follows a certain input $x(t)$ and disturbances on the output $d(t)$ are rejected. The general structure of a closed loop control system is shown in Figure 1.1. To achieve the tracking of the input and the stabilization of the output, a controller $G(s)$ uses the error $e(t)$ to control the plant $P(s)$ accordingly. The error is defined as

$$e(t) = x(t) - r(t) = x(t) - [y(t) * h(t)] \tag{1.30}$$

with $h(t)$ being the inverse Fourier transform of the filters transfer function $H(s)$.

Feedback control systems, or closed-loop systems are to be differentiated from open-loop systems, in which there is no return path, so they cannot compensate for *un*known disturbances. If $d(t)$ is known $\forall t$, then an open loop system would be possible and any errors could simply be compensated.

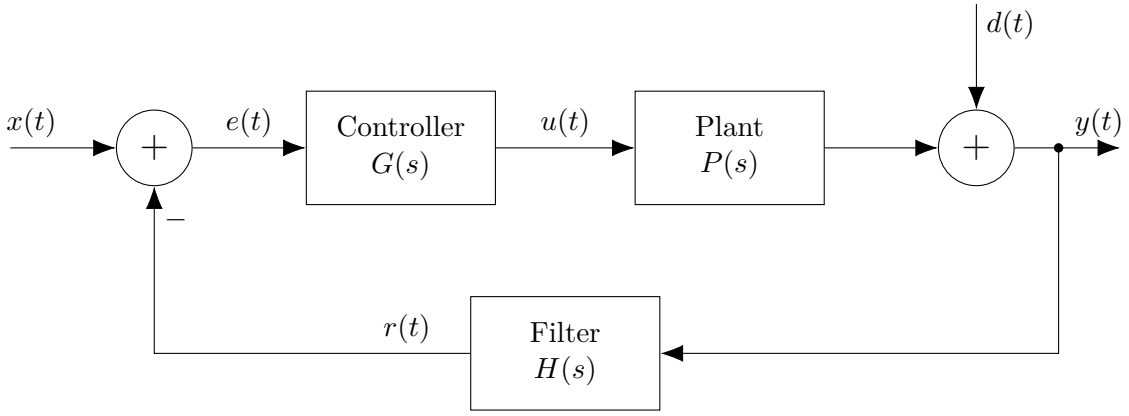

Figure 1.1: General structure of a time continuous feedback control system

1.4.1 Disturbance Rejection and Input Tracking

1.4.2 Stability

Appendix

A Lab Test and Measurement Equipment

A.1 Benchtop multimeters

A.1.1 Agilent 34411A

Table A.1: Agilent 34411A specifications

Specification	**Value**
	DC volt
Digits	6 1/2
Measurement method	cont integrating multi-slope IV A/D converter
Accuracy (10 V range, 24 hours)	0.0015 %+0.0004 % (% of reading + % of range)
Bandwidth	15 kHz (typ.)

Table A.2: Agilent 34411A some SCPI commands

Description	**Example command**	**Example return**
Read current measurement	`READ?`	`+2.84829881E+00` (2.848 V)

A.1.2 Keysight 34470A

Table A.3: Keysight 34470A specifications

Specification	**Value**
	DC volt
Digits	7 1/2
Measurement method	cont integrating multi-slope IV A/D converter
Accuracy (10 V range, 24 hours)	0.0008 %+0.0002 % (% of reading + % of range)
Bandwidth (10 V range)	15 kHz (typ.)

Table A.4: Keysight 34470A some SCPI commands

Description	**Example command**	**Example return**
Read current measurement	`READ?`	`+9.99710196E+00` (9.997 V)

A.2 Data Acquisition/Switch Unit

A.2.1 Keysight 34972A

Table A.5: Keysight 34972A specifications

Specification	Value
34907A (Multifunction module)	
DAC range	±12 V
DAC resolution	16 bit ($^{24\,V}/_{2^{16}}$ = 366.21 µV per bit)
DAC maximum current	10 mA
34901A (20 channel multiplexer)	

Table A.6: Keysight 34972A some SCPI commands

Description	Example command	Example return
Read current measurement	`READ?`	`+2.00200000E+01` (20.02 °C)
Set DAC voltage of ch 204 to 3.1 V	`SOUR:VOLT 3.1,(@204)`	

A.3 Oscilloscopes

A.3.1 Tektronix MSO64

Table A.7: Tektronix MSO64 specifications

Specification	Value
Bandwidth	6 GHz
Sample rate	25 GS/s
ADC resolution	12 bit
DC gain accuracy (@ 50 Ω, >2 mV/div)	±2 %

Table A.8: Tektronix MSO64 some SCPI commands

Description	Example command	Example return
Read mean of measurement 1 (current acq.)	`MEASUrement:MEAS1:RESUlts:CURR:MEAN?`	`3.0685821787408`

A.4 RF signal generator

A.4.1 Rohde and Schwarz SMC100A

Table A.9: Rohde and Schwarz SMC100A specifications

Specification	Value
Frequency range	9 kHz to 3.2 GHz
Maximum power level	17 dBm
SSB phase noise (@ 1 GHz, $f_o = 20$ kHz, $BW = 1$ Hz)	−111 dBc
Level error	<0.9 dB

Table A.10: Rohde and Schwarz SMC100A some SCPI commands

Description	Example command	Example return
Set RF power level to 10.5 dBm	`SOUR:POW 10.5`	
Set RF frequency to 3.1 GHz	`SOUR:FREQ:FIX 3.1e9`	
Enable the RF output	`OUTP on`	

A.5 RF power meter

A.5.1 HP E4419B

Table A.11: HP E4419B specifications

Specification	Value
Digits	4
Accuracy (abs. without power sensor)	±0.02 dB
Power probe: E4412A	
Frequency range	10 MHz to 18 GHz
Power range	−70 dBm to 20 dBm

Table A.12: HP E4419B some SCPI commands

Description	Example command	Example return
Measure power on input 1	`MEAS1?`	`+2.89435802E+000` (2.894 dBm)

A.6 Vector Network Analyzer

A.6.1 Agilent E5071C

Table A.13: Agilent E5071C specifications

Specification	Value
Frequency range	9 kHz to 8.5 GHz

A.7 Phase noise analyzer

A.7.1 Holzworth HA7062C

Table A.14: Holzworth HA7062C specifications

Specification	Value
DUT input frequency	10 MHz to 6 GHz
Measurement bandwidth	0.1 Hz to 40 MHz offsets

Acknowledgments

A

Bibliography

[1] F. Hinterberger, *Physik der Teilchenbeschleuniger und Ionenoptik mit durchgerechneten Beispielen und 99 Übungsaufgaben mit vollständigen Lösungen*. Berlin, Heidelberg, New York: Springer, 1997, ISBN: 9783540612384.

[2] T. Wangler, *RF linear accelerators*. Weinheim: Wiley-VCH, 2008, ISBN: 9783527623426.

[3] K. I. Park, *Fundamentals of Probability and Stochastic Processes with Applications to Communications*. Springer International Publishing, Dec. 4, 2017, 288 pp., ISBN: 3319680749.

[4] F. Puente León, *Messtechnik*. Springer-Verlag GmbH, 2019, ISBN: 3662597667.

[5] A. Lapidoth, *A Foundation in Digital Communication*. Cambridge University Press, Mar. 26, 2019, 920 pp., ISBN: 1107177324.

[6] P. Stoica, *Introduction to spectral analysis*. Upper Saddle River, N.J: Prentice Hall, 1997, ISBN: 0132584190.

[7] D. Rowell. (2008). 2.161 Signal Processing: Continuous and Discrete, Massachusetts Institute of Technology: MIT OpenCourseWare, [Online]. Available: `https://ocw.mit.edu/courses/mechanical-engineering/2-161-signal-processing-continuous-and-discrete-fall-2008/#`.

[8] P. Welch, "The use of fast Fourier transform for the estimation of power spectra: A method based on time averaging over short, modified periodograms'', *IEEE Transactions on Audio and Electroacoustics*, vol. 15, no. 2, pp. 70–73, Jun. 1967. DOI: `10.1109/tau.1967.1161901`.